The effect of climate change and low CO_2-binders on the service life of concrete structures due to carbonation

J.H.M. Visser
TNO, the Netherlands

Carbonation of concrete is strongly affected by local climate conditions but degradation models do not take this fully into account. Hence an updated model is presented including both an extension of the (environmental) loads as well as the resistance of the concrete against these loads. Loads from the environments that are included are CO_2 concentration, relative humidity and time of wetness. The data is based on historical data of the Dutch weather stations across the country, and extrapolated based on the current climate changing trends. The resistance against carbonation has been modelled in more detail by including the principal concrete composition parameters. The climate effects on carbonation have been demonstrated for three types of cement, with a variable amount of calcium content and with a different pore fineness in the hardened state. The results of the modelling indicate a significant increase in carbonation depth for hardened binders that dry out under the current relative humidity. The change in carbonation rate is however dramatic for those cements that currently remain saturated at the prevailing relative humidity but will dry out due to the lower RH as a consequence of climate change. Their carbonation rate increases so much that the service life may be compromised. This first assessment of the climate change effects on carbonation, couples to the drive towards low or no clinker-based binders warrants urgent further research towards the effect of these binders both at the current and the future climate.

Key words: Service life, carbonation, environmental load, material resistance, climate change

1 Introduction

Concrete structures have a technical service life that often exceed their design service life of 50 years or more (fib, 2022). These structures then may be left in service for a longer period than designed for. Other structures may still have a sufficient long remaining service life but may go out of service because of loss of functionality. The components of such a structure (or even the structure as a whole) may be reused rather than demolished. In

contrast, there are also structures that do not reach their design service life as they degrade faster than expected when designed. In all mentioned cases, an accurate prediction of the remaining service life would be required for an assessment of the possibility to leave, reuse, repair or recycle the structure (Visser & Siemes, 2010), (fib MC2020 Task group 3.2, 2020).

The service life of a structure is determined by that degradation mechanism that fails its requirement(s) soonest (DuraCrete, 1998), (DuraCrete, 2000), (fib MC2020 Task group 3.2, 2020). These requirements in general are written down in the form of limit states, e.g. with respect to carbonation it states that the probability P that the depth of carbonation exceeds the cover depth within the required service life should be smaller than P_{acc}:

$$P\{x_c(t_{SL}) - d_c > 0\} < P_{acc} = \Phi(-\beta) \quad (1)$$

In which P_{acc} is the a-priori agreed upon probability of corrosion initiation, x_c is the carbonation front, d_c is the cover depth and t_{SL} is the service life. The probability of corrosion initiation P_{acc} can be furthermore be expressed in terms of the reliability index β with Φ the probability distribution function. The rate with which the carbonation front reaches its limit state is described by a degradation model (Alexander & Beushausen, 2019; Fédération Internationale du Béton (fib), 2010; fib, 2013), (DuraCrete, 2000), (Gehlen & Capteina, 2004). Thus, one of the prerequisites of a reliable degradation model is that it contains all variables that have a noticeable effect on the rate of degradation. In the case of the carbonation process, it is known that it depends both on the material properties (e.g. permeability, CO_2-binding capacity) that define the resistance against carbonation and the environmental loads such as rain fall, relative humidity and temperature.

Portland cements are known to have a high resistance against carbonation due to their high CO_2-binding capacity and formation of reaction products that block the pores for further degradation (Visser, 2014), (Thiery et al., 2005), (Leemann & Moro, 2017). With the drive towards more sustainable cements, however, Portland cement use in concrete is reducing as it is tried to have blends with as high amount of secondary binders such as fly ash, slag and calcium carbonate as possible. Recently also calcined clays and other lower CO_2-generating supplementary materials are used. These materials have in common that they have lower calcium-content which results in less of no formation of calcium phases that can carbonate and/or block the pores in concrete, such as $Ca(OH)_2$ (Visser, 2014), (Shi

et al., 2016), (von Greve-Dierfeld et al., 2020). On the other hand, these materials in general have a smaller pore size, which results in higher degrees of saturation of the concrete at similar ambient relative humidity. Saturated pores prevent CO_2 to penetrate the concrete, as the transport of CO_2 through water is much slow (more than ca 10.000, see e.g. (Lyde, 2003),(Sposito, 2004)). However, climate change may result in many areas in long(-er) dry periods at low relative humidity, resulting in faster drying out of concrete and thus at a higher carbonation rate. Performance of materials cannot be deducted from past experience anymore but have to be amended for the new environmental load conditions. This paper explains how the environmental loads influence the service life and how this affect the sustainability of the concrete structures, as this low CO_2-binder choice and climate load changes are in obvious conflict. An illustration of the effect is given on the basis of an average value calculation.

2 Degradation model for carbonation

The carbonation depth at any point in time $x_c(t)$ is expressed by:

$$x_c(t) = W(t)\, k \sqrt{t} \tag{2}$$

with $W(t)$ the weather function, k is an empirical factor and t the exposure time. This model is used in the *fib* MC2020 (fib, 2022). With reference to *fib* Bulletin 34 (Fédération Internationale du Béton, fib, 2010), the empirical factor k is further specified as:

$$k = \sqrt{k_e\, k_c (k_t R_{carb}^{-1} + \varepsilon_t)\, c_s} \tag{3}$$

in which c_s is the CO_2-concentration, R_{carb} is the resistance against carbonation and ε_t is the uncertainty in the test results when not using a Natural Carbonation (NC-) test. The three k-factors are curing factor k_c , environmental factor k_e and test factor k_t . The test factor k_t = 1 for the NC-test and the curing factor k_c = 1 for standard curing. In this paper, only k_e will be discussed further. For the influence of curing time and temperature, see e.g. (Yeon & Kim, 2025)

2.1 The CO_2 concentration at the surface cs

The CO_2-concentration in the ambient air is increasing (see Figure 1) To first order, it can be described by a linear function:

$$c_s(t) = c_s(T_{ref}) + A_{cs}t \tag{4}$$

and extrapolated under assumption that the increase in CO_2 cannot be put on hold and a linear increase being the worse-case scenario. With the current CO_2 level c_s (T_{ref} = 2023) being 414 ppm (Figure 1), and A_{cs} = 1.9 ppm/year, this would mean that in 50 years, the CO_2 concentration is already 508 ppm.

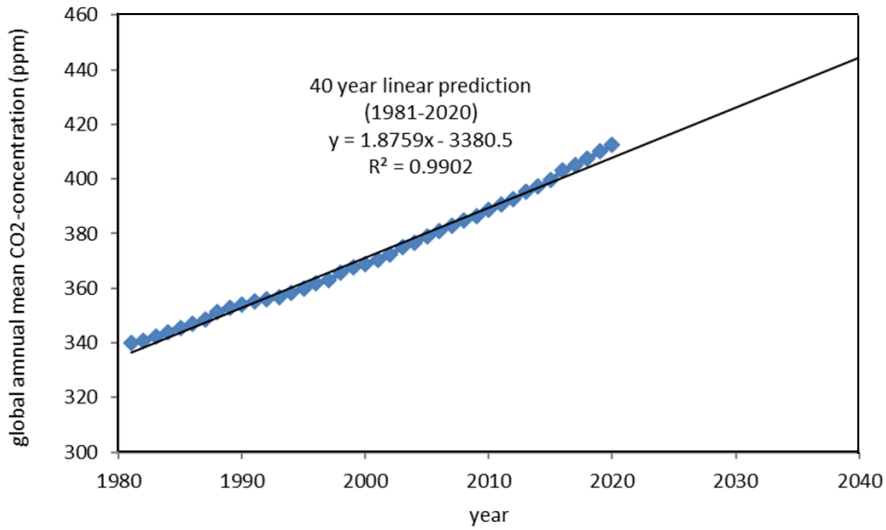

Figure 1. Predicted CO_2 increase on earth for the coming decennia
Data from ftp://aftp.cmdl.noaa.gov/products/trends/co2/co2_annmean_gl.txt , accessed 2023 02 15

2.2 ***The environmental function***

The environmental function k_e includes the effect the ambient relative humidity on the carbonation of the concrete. This makes it a material parameter, rather than an environmental parameter. It does contain, however, also the local relative humidity as variable. In the *fib* MC2020, the relative humidity–carbonation rate dependency has been modelled with help of an empirical model that has no physical explanation. However, in this paper a more physically based model is used:

$$k_e(RH) = \begin{cases} \left(1 - \dfrac{(RH(t) - RH_{MC})^2}{(RH_{MC})^2}\right) \Big/ \left(1 - \dfrac{(RH_{ref} - RH_{MC})^2}{(RH_{MC})^2}\right) & \forall \quad RH \le RH_{MC} \\ \left(1 - \dfrac{(RH(t) - RH_{MC})^2}{(RH_{sat} - RH_{MC})^2}\right) \Big/ \left(1 - \dfrac{(RH_{ref} - RH_{MC})^2}{(RH_{sat} - RH_{MC})^2}\right) & \forall \quad RH > RH_{MC} \end{cases} \tag{5}$$

In which $RH(t)$ is the yearly average relative humidity at year t and RH_{sat} denotes the relative humidity at which the concrete becomes fully saturated and carbonation thus stops. RH_{MC} is the relative humidity at which the carbonation rate is maximum. The function is scaled to its value at a RH_{ref} = 65 %, at which the natural carbonation test is executed so that at this standard condition k_e = 1 as required. Some modelling results based on laboratory carbonation data are shown in Figure 2.

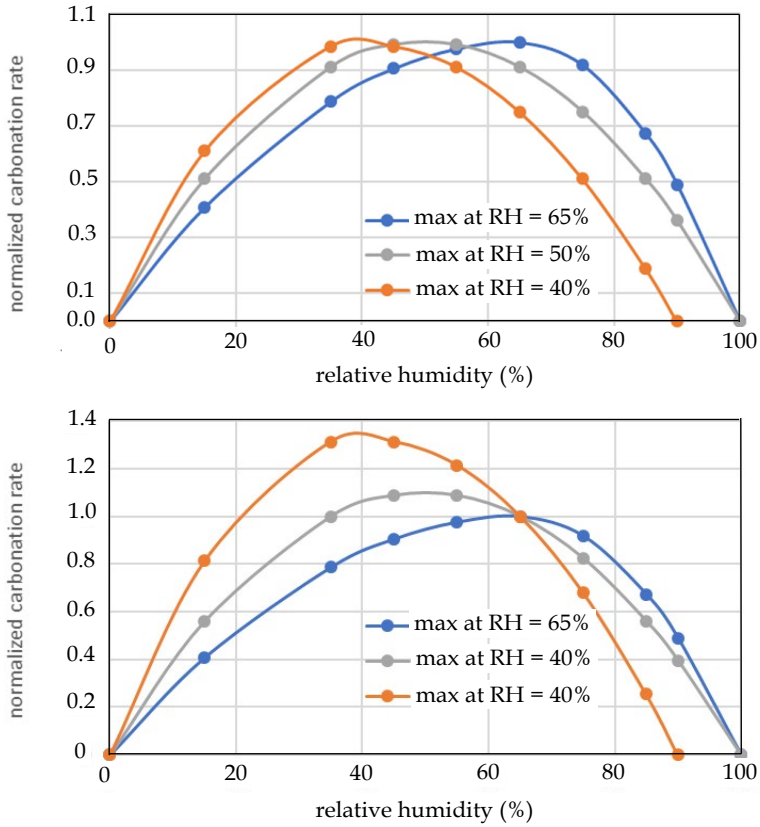

Figure 2. Carbonation rate as function of the relative humidity function Equation 10 normalized on the maximum rate (top); and normalized the rate at RH = 65% to have k_e = 1 at the NC-condition of RH = 65% (bottom). Data is measured carbonation points from (Verbeck, G., and Gramlich, 1955), (Thiery et al., 2005), (V.G. Papadakis et al., 1991)

The local relative humidity determines whether carbonation will take place and how fast: in a dry environment, the carbonation will go much faster for most binders than measured

at the laboratory relative humidity of 65%. It can be taken from the nearest local weather station. A prediction of the (yearly mean) relative humidity can be obtained from the 20-year running means relative humidity as shown in Figure 3 at three different weather stations in the Netherlands showing the same decrease in *RH*. Based on this 20-year running average, the (20-year running) yearly mean relative humidity can be modelled as:

$$RH(t) = RH(T_{ref}) - A_{RH}\, t \tag{6}$$

With T_{ref} = 2023, $RH(T_{ref})$ = 79.1 and A_{RH} = 0.17%/year for the Schiphol location, for instance. If it is assumed that the historic trend will continue the next years, the *RH* will decrease e.g. at Schiphol from 79% to 70% in 50 years.

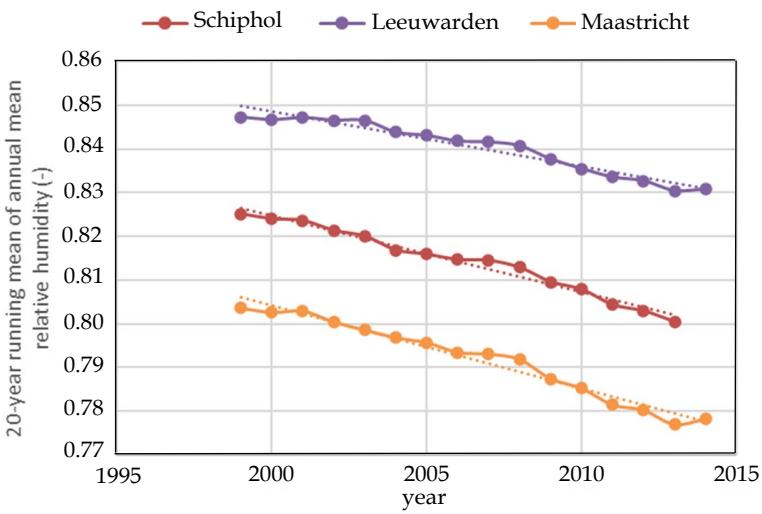

Figure 3. 20-yr running mean of the yearly mean relative humidity of 3 Dutch weather stations
Data from: Climate Explorer: Running mean (knmi.nl)

2.3 ***Weather function***

The weather function *W*(*t*) is a decaying function according to:

$$W(t) = \left(\frac{t_0}{t}\right)^{\frac{w}{2}} \tag{7}$$

With t_0 the reference time, usually taken as the age of which exposure starts, and t the exposure time. The factor w is called weather exponent and takes the local weather (meso-climate) into account:

$$w = (P_{wind} P_{rain} P_{orientation})^{b_w} \quad (8)$$

with

P_{wind} …….. Probability of a windy day > 2 m/s at a location [-]

P_{rain} …….. Probability of more than 1 mm rain at a location [-]

$P_{orientation}$ .. Probability of prevailing wind on surface in a 120 degree wind window [-]

b_w …….. Exponent of regression [-]

The probabilities are real numbers between 0 and 1. P_{rain} is the period in which sufficient wetness is fallen to likely saturate the concrete. When wet, carbonation cannot progress. It is defined here as the probability that during a day more than 1 mm rain falls, regardless the orientation of the surface. It is based on historic data from the nearest weather station at a certain location. Similarly, P_{wind} is the period in which the wind blows sufficiently hard to drive the rain towards a surface. 'Sufficient' has been defined as a wind speed of

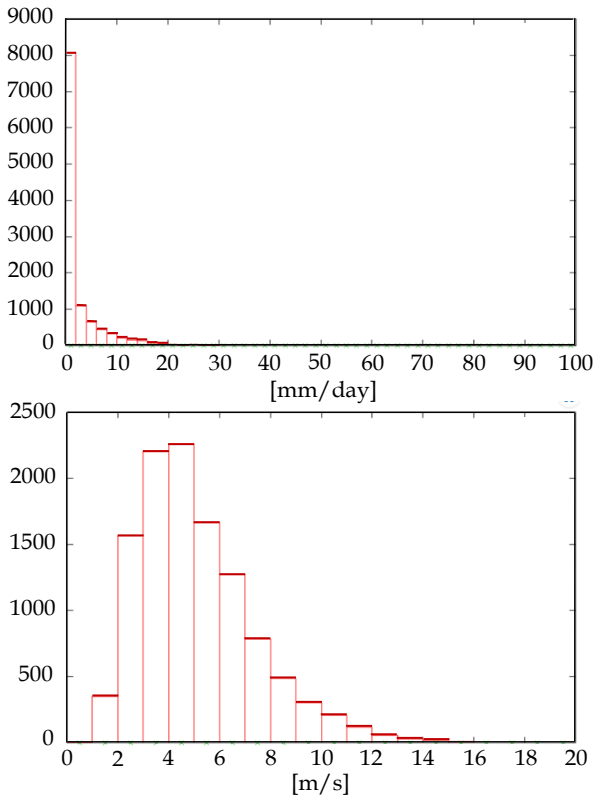

Figure 4 Examples of the distribution of the amount of rain per day (top) and average wind speed per day (bottom) between 1990-2020 at the Schiphol weather station. Data from www.knmi.nl

more than 2 m/s. Also this probability can be determined from historical data from the nearest weather station. For the Schiphol area, the probability of wind > 2 m/s is 0.96, the probability of a rainy day > 1 mm is 0.28.

The probability of wetting a surface depends on the orientation of the facades to the wind. Figure 5 shows the probability of a prevailing wind direction in the Netherlands at the Schiphol weather station. As a practical rule, the driving rain is taken into account for the wind direction perpendicular to the façade, +/- 60 degrees, as rain driven more or less parallel to the surface also will hardly wet the surface. For the Schiphol area, this means that e.g. North orientated facades have only half the change of getting wet than at the S-SW orientation (0.25 versus 0.5). In addition, horizontal surfaces always get wet, so $P_{orientation}$ = 1 for horizontal surfaces and 0 for sheltered or indoor locations.

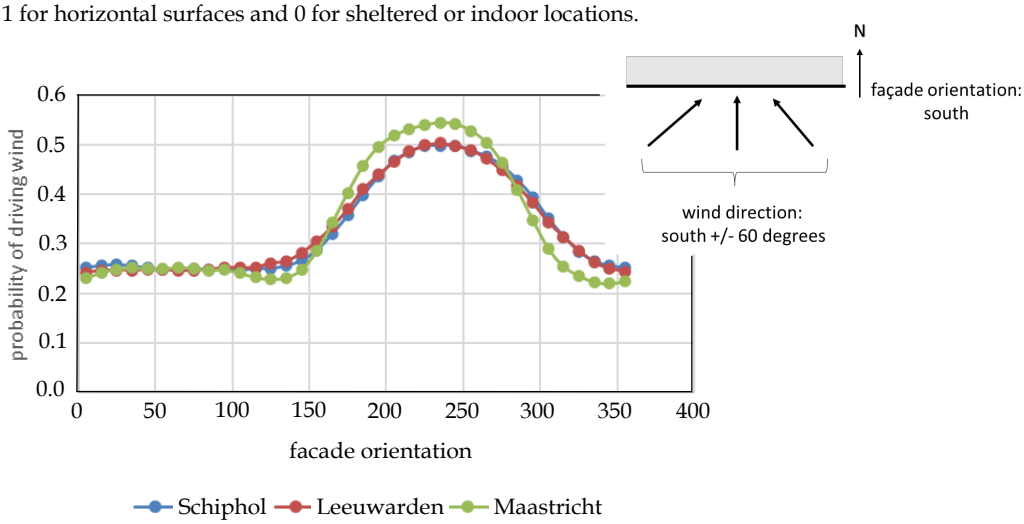

Figure 5. Example of the probability of wind on façade at the three Dutch weather station depending on the wind orientation; example for south orientated façade at driving rain from west to southwest to east south east wind directions, wind direction 0 degrees = North

The model implies that the rainy days, windy days and prevailing wind are independent. This is in general not the case. The prevailing wind at Schiphol can be seen to be west-south west. Since the wind comes then comes from the North sea, it can be expected to bring most of the time rain. Winds from the east blow more often without rain. A full coupling of the databases of the rainfall > 1mm, wind speeds > 2 m/s and orientation thus is required, but as a first assessment, the probability of driving rain is taken as the products of three parameters as indicated by Equation 7. On the basis of the historical data at the

weather station, no trend can be observed with respect to changes in prevailing wind direction, mean daily wind or daily precipitations. The probability of driving rain and time of wetness are therefore taken as time independent.

The final parameter in the weather function is the regression parameter b_w , which is basically the calibration factor that ultimately finetunes the square-root time behavior to the actual carbonation front progress for a certain local climate, according to Equation 5. The resulting time dependent carbonation behaviour, including dry and wet periods is bound on [0, 1]: for $w = 0$, there is no weather effect. This situation applies for indoors or outdoors/sheltered situations. The carbonation front then describes its 'classical' square-root time progression with time. For $w = 1$, there is no carbonation from progress with time. This situation applies to permanent wet conditions. In all other cases, it is expected that the square-root behaviour is reduced, which implies that $0 < w < 1$. The regression parameters b_w is therefore a positive number. The input for the weather function is given in Table 1.

Table 1. Input for the weather function w

Orientation	w	$P_{orientation}$
Indoors	0	-
Outdoors/sheltered	0	-
Outdoors/unsheltered	From Equation 8 and Table 2	Horizontal = 1 Vertical from Figure 5
Submerged	1	-

Table 2. Input for the location dependent parameters

Region NL	Location	Time dependent RH (Eq. 6)		P_{wind}	P_{rain}
		RH_{ref}	A_{RH}		
North	Leeuwarden	82.0	0.13	0.962	0.290
Mid, coast	Schiphol	79.1	0.17	0.964	0.287
South, land	Maastricht	75.6	0.19	0.940	0.262

2.4 *The resistance against carbonation* R_{carb}

The resistance against carbonation is measured in a so-called Natural Carbonation (NC-) test (in the laboratory), at which specimens are conditioned at 65% relative humidity and 20˚C but otherwise ambient air. The resistance measured in this environmental load is chosen as the standard resistance. The carbonation depth equation in the NC-test becomes:

$$x_c(t) = \sqrt{\frac{c_s t}{R_{carb}}} \tag{9}$$

with R_{carb} being the resistance of the material against carbonation in the NC test being equal to:

$$R_{carb} = \frac{a}{D_{carb}} \tag{10}$$

In which a is the CO_2-binding capacity (determined by the amount of calcium that can be supplied by the cement paste to neutralize the penetrating CO_2, given the chemical equilibrium conditions) and D_{carb} is the diffusion coefficient of CO_2 in the carbonated concrete. Amongst others, the resistance against carbonation of concrete depends on the type of cement and the water-to-cement ratio (see Figure 6).

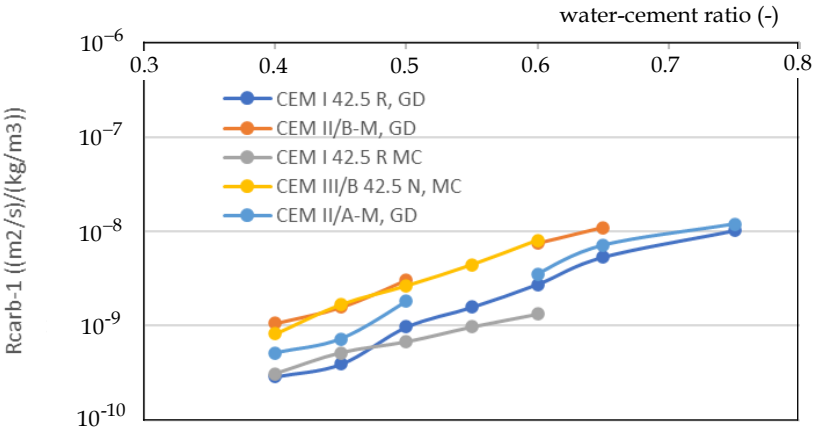

Figure 6. Measured carbonation conductivity $R_{carb}^{-1} = D_{carb}/a$

Data from GD (von Greve-Dierfeld et al., 2020) and MC (fib, 2013)

The resistance against carbonation can also be calculated from Equation 10, in which the CO_2-binding capacity a can be estimated from the cement content per cube of concrete and the relative amount of calcium in the cement (%CaO) by means of :

$$a = k_a \%CaO = 0.7\ C\ Ca \quad (11)$$

with k_a is a conversion factor (kg Ca/m³ concrete)/(%CaO/kg cement), to convert the relative calcium content (in %CaO/kg cement) to the CO_2-binding capacity (in kg Ca/m³ concrete), depending on the amount of cement used per m³ concrete (280 kg/m³ to 450 kg/m³). The factor can be estimated from the concrete composition, taking all calcium in the cement into account but excluding phases already present as calcium carbonate. It can also be measured from the amount of CO_2 that concrete can take up.

The diffusion coefficient of CO_2 in carbonated concrete can be measured directly (or indirectly by e.g. N_2 , see Dutzer et al., 2019). The diffusion coefficient with respect to CO_2 is for the carbonated concrete, since CO_2 diffuses to the carbonation front through already carbonated concrete. To first order, all cement types have the same relationship between diffusion coefficient and the water-to-cement ratio:

$$D_{carb} = D_{ref} \exp A(wcr - wcr_{ref}) \quad \text{with } 0.4 < \text{wcr} < 0.75 \quad (12)$$

With the averaged fitted model, choosing wcr_{ref} as 0.4 resulting in increasing diffusion coefficients for CO_2 in the carbonated concrete, ranging from 8 10^{-8} m²/s for CEM I and 44 10^{-8} m²/s for CEM III/B (Figure 7).

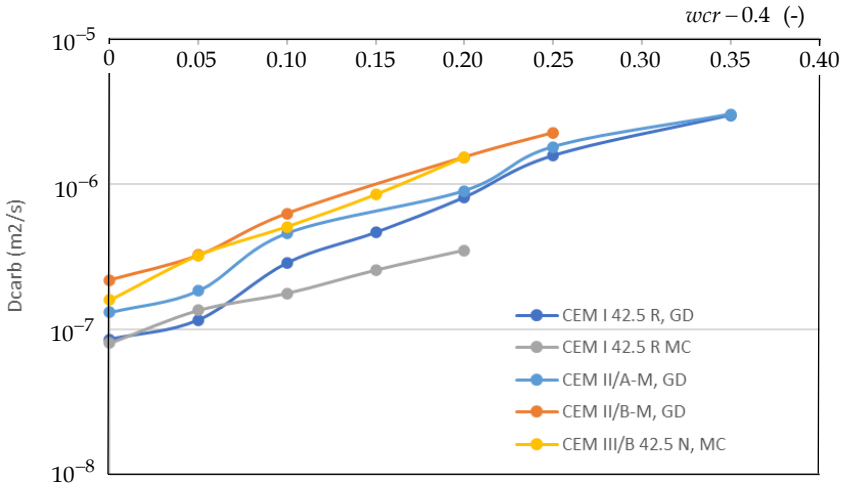

Figure 7. Relationship between diffusion coefficient in the carbonated concrete and $wcr - wcr_{ref}$ = wcr – 0.4 and fit parameters according to Equation 18, for estimated a on the basis of cement type and average cement amounts for MC of 400 kg/m³ and GD of 450 kg/m³ for GD as reported. Data from GD (von Greve-Dierfeld et al., 2020) and MC (fib, 2013)

Table 3. Data on Figure 7

Binder	D_0 (10^{-8} m²/s)	A (-)	R_2
CEM I (MC)	9	10.8	0.965
CEM I (GD)	9	7.1	0.994
CEM II/A-M	14	9.3	0.956
CEM II/B-M	22	9.6	0.956
CEM III/B	44	11	0.998

The influence of the concrete composition as function of the cement type on the buffering capacity and the diffusion coefficient is shown in Figure 8, based on Equation 11 and 12, from the data from Figure 6 and 7. In the figures, it can be seen clearly that the buffering capacity of the low clinker binders is greatly reduced while at the same time the diffusion coefficient increases.

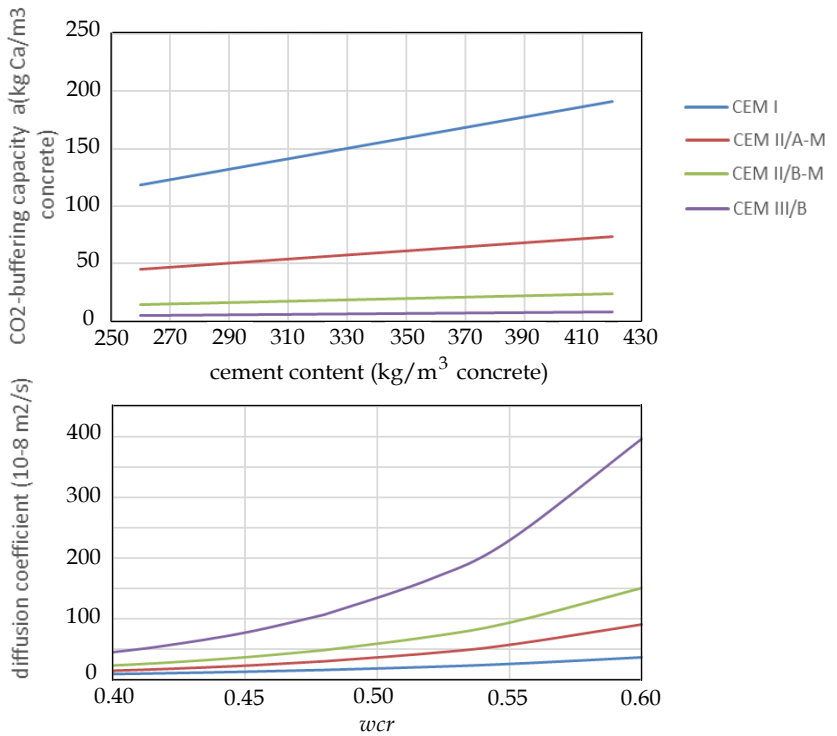

Figure 8. Relationship between diffusion coefficient in the carbonated concrete and wcr – wcr_{ref} = wcr – 0.4 and fit parameters according to Equation 18, for estimated a on the basis of cement type and average cement amounts for MC of 400 kg/m³ and GD of 450 kg/m³ for GD as reported

In addition to the *wcr*, the diffusion coefficient of CO_2 in concrete can be expected to depend on the ratio cement paste/aggregates, with higher amount of paste giving thus higher amounts of pores. To first order this effect can be introduced by a scaling factor like, e.g. the cement /aggregate factor. However, by expressing both the diffusion coefficient and the CO_2 binding capacity per cubic meter concrete, this effect is eliminated in the resistance of concrete against carbonation (Eq. 9). Hence, in addition to the measured resistance against carbonation, it can be estimated by:

$$R_{carb} = \frac{a}{D_{ref} \exp A(wcr - wcr_{ref})} \qquad \text{with } 0.40 < wcr < 0.75 \tag{13}$$

The input table for various binders is given in Table 4. Further refinement of the material properties is possible, e.g. by using composed binder models to predict the diffusion coefficient (Rathnarajan & Pillai, 2025) but fall out of the scope of this paper.

Table 4. Input table for binder parameters; range of wcr = 0.4 – 0.75 and kg cement/m³ concrete = 280 – 400 kg/m³

Binder	CaO (wt-%)	D_{ref} (10^{-8} m²/s)	A (-)	RH_{MC}	RH_{sat}
CEM I	65	9	11 / 7	65	100
CEM II/A-M	55	14	9.3	65	100
CEM II/B-M	46	22	9.6	65	100
CEM III/B	48	44	11	40	85

3 The influence of climate change on the carbonation rate

To demonstrate the influence of the climate change on the carbonation rate, the progress of the carbonation front have been run for illustration, taking into account the increase of the CO_2-concentration c_s and the decrease in relative humidity *RH*. In addition, to take into account the effect of the concrete composition, cements with a different amount of clinker and concrete with different cement contents have been included as well. Figure 9 top shows the results for CEM I (100% clinker) and CEM II/A-M (ca 70% clinker) at 260 kg cement/m³ concrete and 420 kg cement/m³ concrete. The results show that decreasing the amount of cement per m³ concrete as well as decreasing the amount of clinker in cement increases the carbonation rate. However, the climate change effect is more or less similar

for the two types of cement, mostly due to the fact that the cements have the same relative humidity for which the carbonation rate is maximum and the same relative humidity for which the concrete becomes saturated (and carbonation thus stops). Figure 9 bottom shows the impact on the carbonation depth for CEM III/B (30% clinker, 70% slag). The concrete is saturated at ca. 85% which is also the average relative humidity in the Netherlands. This implies that carbonation of most structures in the Netherlands at the moment do not suffer much from carbonation due to the wet conditions. When the average relative humidity becomes lower that the saturation relative humidity, the blast furnace slag cement start to dry out and thus is able to carbonate. This effect accelerated with time due to the ongoing decrease in *RH*, as shown in Figure 3. The effect is devasting: instead of a carbonation resistance in service that is close to that of CEM I, it becomes incredibly much worse.

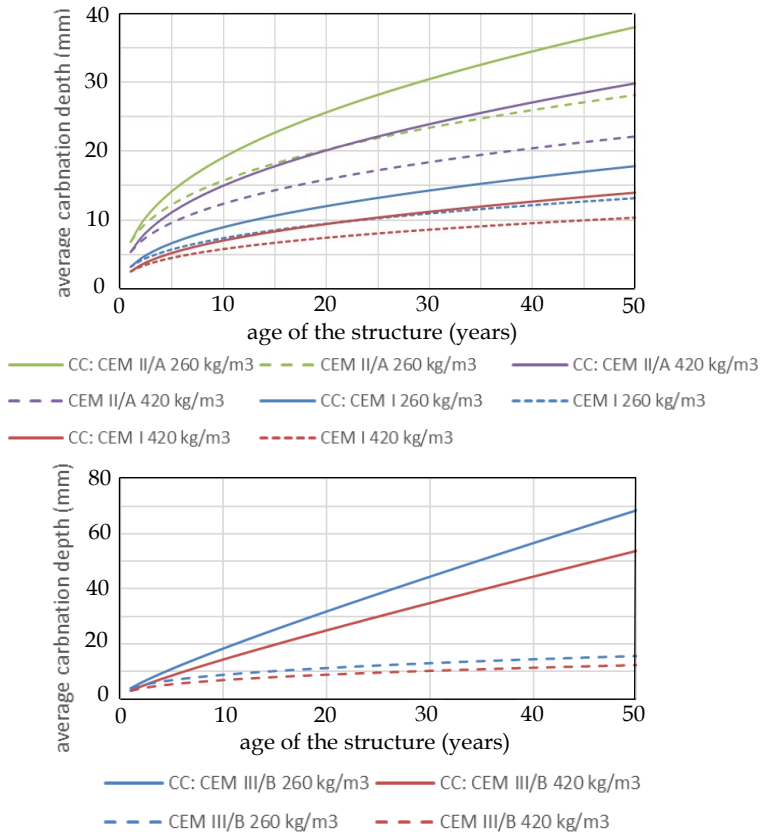

Figure 9. Average carbonation depth progress with time with and without climate change included. Model calculations based on the Schiphol climate data, South facade: CEM I and CEM II/A (top) and CEM III/B (bottom). CC = scenarios with climate change included

4 Conclusions

It has been demonstrated in this paper that carbonation of concrete is strongly affected by the climate conditions. Based on the historical data of the Dutch weather stations, it was found that the long-term average of the mean annual relative humidity is steadily decreasing. If this decrease will continue, the average relative humidity in the Netherlands is substantially decreasing over the next 50 - 100 years by more than 10%. Prevailing wind and rain fall could not been seen to change during the last 20 years across the country and thus have been taken as constant. As a result, the drying of concrete will be more sever in the future, giving rise to faster carbonation.

The model calculations that have been presented as illustration show for instance that for CEM I after 50 years, the average carbonation depth is 14 - 18 mm of CEM I concrete at a *wcr* of 0.45 depending on the cement content and for a relative dry south façade. Climate change has little effect: a 4 - 5 mm additional increase in carbonation depth after 50 years. The resistance against carbonation for CEM II/A is much lower (30 - 38 mm), and the effect of the climate change consequently higher (8 - 10 mm in addition after 50 year). The most dramatic effect is however for those binders that up to now remain saturated under the current climate conditions but will dry out if the climate change is not stopped. Then, their low resistance against carbonation takes effect. This has been demonstrated for CEM III/B. At the current climate conditions, the average carbonation depth is like that of CEM I but increase to 50 - 70 m after 50 years in the simulated climate change conditions. On these data it can also be assessed that the probability that carbonation reaches the reinforcement is just several years, instead of 50 years.

When not considering the expected climate change, the preferential use of CEM III/B as cement in the Netherlands may prove to lead to unexpected low service lives for newly designed structures and requires intensified monitoring for existing structures to be able to take early maintenance measures if required. In addition, the current drive of the concrete industry to reduce the clinker content in the concrete mix to mitigate their impact on climate change. Most of these binders have a much lower CO_2 buffer capacity and in general show also an increase in pore size and porosity after carbonation making them susceptible to drying at higher ambient RH. This first assessment of the climate change effects on carbonation, coupled to the drive towards low or no clinker-based binders warrants urgent further research towards the effect of these binders at the current and

future state of the climate. As Radovic et al. (Radović et al., 2024) and von Greve et al. (von Greve-Dierfeld et al., 2020) already shown for the laboratory results (in NC, AC or natural condition testing), carbonation rates increase with cement replacement. However, the results should be coupled to relative humidity changes which is not possible with the current performance models as in the design codes used today.

References

Alexander, M., & Beushausen, H. (2019). Durability, service life prediction, and modelling for reinforced concrete structures – review and critique. *Cement and Concrete Research*, 122 (May), 17–29. https://doi.org/10.1016/j.cemconres.2019.04.018

DuraCrete. (1998). DuraCrete. "Modelling of degradation, DuraCrete–Probabilistic performance-based durability design of concrete structures". In: *EU-BriteEuRam III*, Contract BRPR-CT95-0132,.

DuraCrete. (2000). Statistical Quantification of the Variables in the Limit State Functions.

Dutzer, V., Dridi, W., Poyet, S., Bescop, P. Le, & Bourbon, X. (2019), The link between gas diffusion and carbonation in hardened cement pastes. *Cement and Concrete Research*, 123 (June), 105795. https://doi.org/10.1016/j.cemconres.2019.105795

Fédération Internationale du Béton (fib). (2010). Bulletin 34 - Model Code for Service Life Design.

fib. (2013). Code-type models for structural behaviour of concrete. State-of-the-art report. fib, Lausanne, Switserland.

fib. (2022). The fib Model Code for Concrete Structures 2020.

fib. (2013). Code-type models for structural behavior of concrete. State-of-the-art report. fib, Lausanne, Switserland.

fib MC2020 Task group 3.2. (2020). Modelling of structural performance of existing concrete structures State of the Art Report (Issue Final Draft Aug 31th 2020).

Gehlen, C., & Capteina, G. (2004). DARTS T2.1: Deterioration Modelling.

Leemann, A., & Moro, F. (2017). Carbonation of concrete: the role of CO_2 concentration, relative humidity and CO_2 buffer capacity. *Materials and Structures/Materiaux et Constructions*, 50 (1). https://doi.org/10.1617/s11527-016-0917-2

Lyde, D. R. (2003). *CRC Handbook of Chemistry and Physics*.

Radović, A., Carević, V., Marinković, S., Plavšić, J., & Tešić, K. (2024). Prediction model for calculation of the limestone powder concrete carbonation depth. *Journal of Building Engineering*, 86 (February). https://doi.org/10.1016/j.jobe.2024.108776

Rathnarajan, S., & Pillai, R. G. (2025). Carbonation models using mix-design parameters for concretes with supplementary cementitious materials. *Journal of Building Engineering*, 104(January), 112392. https://doi.org/10.1016/j.jobe.2025.112392

Shi, Z., Lothenbach, B., Rica, M., Kaufmann, J., Leemann, A., Ferreiro, S., & Skibsted, J. (2016). Experimental studies and thermodynamic modeling of the carbonation of Portland cement , metakaolin and limestone mortars,. *Cem. Concr. Res*., 88, 60–72. https://doi.org/10.1016/j.cemconres. 2016.06.006.

Sposito, G. (2004). *The Chemistry of Soils* (1st ed.). Oxford University Press.

Thiery, M., Dangla, P., Villain, G., & Platret, G. (2005). A prediction model for concrete carbonation based on coupled CO_2-H_2O-ions transfers and chemical reactions. *10DBMC International Conférence On Durability of Building Materials and Components* .

Papadakis,V.G. , Vayenas, C. G., & Fardis, M. G. (1991). Fundamental modelling and experimental investigation of concrete carbonation. *ACI Mater.J.*, 88, 363–373.

Verbeck, G., and Gramlich, C. (1955). Osmotic Studies and Hypothesis Concerning Alkali-Aggregate Reaction. *Proceedings of the American Society for Testing and Materials*, 55, 1110–1131.

Visser, J. H. M. (2014). Influence of the carbon dioixde concentration on the resistence to carbonation of concrete. *Construction and Building Materials*, 67, 8–13.

Visser, J. H. M., & Siemes, A. J. M. (2010). *Levensduurberekeningen voor Betonconcstructies*, (Issue ISBN 978-90-5986-345-3).

von Greve-Dierfeld, S., Lothenbach, B., Vollpracht, A., Wu, B., Huet, B., Andrade, C., Medina, C., Thiel, C., Gruyaert, E., Vanoutrive, H., Saéz del Bosque, I. F., Ignjatovic, I., Elsen, J., Provis, J. L., Scrivener, K., Thienel, K. C., Sideris, K., Zajac, M., Alderete, N., … De Belie, N. (2020). Understanding the carbonation of concrete with supplementary cementitious materials: a critical review by RILEM TC 281-CCC. In *Materials and Structures/Materiaux et Constructions* (Vol. 53, Issue 6). https://doi.org/10.1617/s11527-020-01558-w

Yeon, Y., & Kim, J. H. J. (2025). Development of 3D satisfaction surface for concrete durability design under chloride attack considering climate change. *Case Studies in Construction Materials*, 22 (February), 140353. https://doi.org/10.1016/j.cscm.2024.e04181